

EVOLUTIONARY BIOLOGY

Growing up *Tyrannosaurus rex*: Osteohistology refutes the pygmy “*Nanotyrannus*” and supports ontogenetic niche partitioning in juvenile *Tyrannosaurus*

Holly N. Woodward^{1*}, Katie Tremaine^{2,3}, Scott A. Williams³, Lindsay E. Zanno^{4,5}, John R. Horner⁶, Nathan Myhrvold⁷

Despite its iconic status as the king of dinosaurs, *Tyrannosaurus rex* biology is incompletely understood. Here, we examine femur and tibia bone microstructure from two half-grown *T. rex* specimens, permitting the assessments of age, growth rate, and maturity necessary for investigating the early life history of this giant theropod. Osteohistology reveals these were immature individuals 13 to 15 years of age, exhibiting growth rates similar to extant birds and mammals, and that annual growth was dependent on resource abundance. Together, our results support the synonymization of “*Nanotyrannus*” into *Tyrannosaurus* and fail to support the hypothesized presence of a sympatric tyrannosaurid species of markedly smaller adult body size. Our independent data contribute to mounting evidence for a rapid shift in body size associated with ontogenetic niche partitioning late in *T. rex* ontogeny and suggest that this species singularly exploited mid- to large-sized theropod niches at the end of the Cretaceous.

INTRODUCTION

After the publication of its discovery from the famous Hell Creek Formation (HCF) in 1905, the carnivorous dinosaur *Tyrannosaurus rex* (1) was met with intense scientific interest and public popularity, which persists to the present day (2). Numerous hypotheses concerning *T. rex* biology and behavior result from decades of research primarily focused on skeletal morphology and biomechanics [e.g., (3) and references therein]. Only within the past 15 years has bone histology been applied to investigate the aspects of *T. rex* life history inaccessible from gross examinations, addressing questions concerning ontogenetic age, growth rate, skeletal maturity, and sexual maturity. In 2004, two teams independently assessed the growth dynamics of *T. rex* using osteohistology. Their results suggest that *T. rex* had an accelerated growth rate compared with other tyrannosaurids and achieved adult size in approximately two decades (4, 5). The teams focused on growth curves, rather than on detailed analyses or interpretations of bone tissue microstructures. However, osteohistology is critical for establishing a baseline against which skeletal maturity and growth changes in cortical morphology related to life events in this taxon can be tested. Identifying the timing of growth acceleration and empirically quantifying juvenile *T. rex* growth rates are of special importance because the juvenile growth record is lost in older individuals because of bone remodeling and resorption (4, 5).

Here, we examine the femur and tibia bone microstructure of two tyrannosaur skeletons of controversial taxonomic status recovered from the HCF: BMRP (Burpee Museum of Natural History) 2002.4.1,

a largely complete specimen composed of nearly the entire skull and substantial postcranial material, and BMRP 2006.4.4, a more fragmentary specimen. Respectively, we estimate these specimens to be 54 and 59% the body length of FMNH (Field Museum of Natural History) PR 2081 (“Sue”) (6, 7), one of the largest known *T. rex*. The ontogenetic age of BMRP 2002.4.1 was previously reported by Erickson (8) as 11 years based on fibula osteohistology. However, because the fibula grows more slowly than the weight-bearing femur and tibia, it does not reflect annual increases in body size or relative skeletal maturity as accurately [e.g., (9)]. We use femur and tibia data to (i) provide detailed comparative intra- and interskeletal histological descriptions, (ii) quantify the ontogenetic age and relative skeletal maturity of these specimens, and (iii) allow empirical observation of annual growth rate, with emphasis on variability during the life history of tyrannosaurs (10).

Moreover, by histologically quantifying the ontogenetic age of BMRP 2002.4.1 and BMRP 2006.4.4 and inferring skeletal maturity, we present new data that can be used to evaluate competing taxonomic hypotheses regarding these and other mid-sized tyrannosaur specimens discovered in the HCF, specifically whether BMRP 2002.4.1 (and by proxy other specimens) represents an adult “pygmy” genus of tyrannosaurid, “*Nanotyrannus*.”

RESULTS

For detailed, orientation-specific histology descriptions, refer to the Supplementary Materials. In general, the femur and tibia cortical bones of BMRP 2002.4.1 and BMRP 2006.4.4 can be classified as a woven-parallel complex. Vascularity and osteocyte lacuna density are uniformly high throughout (Figs. 1 and 2). In the femora, the primary and secondary osteons surrounding vascular canals are frequently isotropic in the transverse section (Fig. 1, A and B) and anisotropic in the longitudinal section (Fig. 1C). Also in the transverse section, femur primary tissue exhibits moderate anisotropy regionally and weak anisotropy locally, corresponding to a loose arrangement of mineralized fibers in parallel (e.g., Fig. 1, A and B, and fig. S3B).

¹Department of Anatomy and Cell Biology, Oklahoma State University Center for Health Sciences, 1111 W. 17th St., Tulsa, OK 74104, USA. ²Department of Earth Science, Montana State University, P.O. Box 173480, Bozeman, MT 59717, USA. ³Museum of the Rockies, Montana State University, 600 W. Kagy Blvd., Bozeman, MT 59717, USA. ⁴Paleontology, North Carolina Museum of Natural Sciences, 11 W. Jones St., Raleigh, NC 27601, USA. ⁵Department of Biological Sciences, North Carolina State University, 3510 Thomas Hall, Campus Box 7614, Raleigh, NC 2769, USA. ⁶Chapman University, 1 University Dr., Orange, CA 92866, USA. ⁷Intellectual Ventures, 3150 139th Avenue Southeast, Bellevue, WA 98005, USA.

*Corresponding author. Email: holly.ballard@okstate.edu, holly.n.woodward@gmail.com

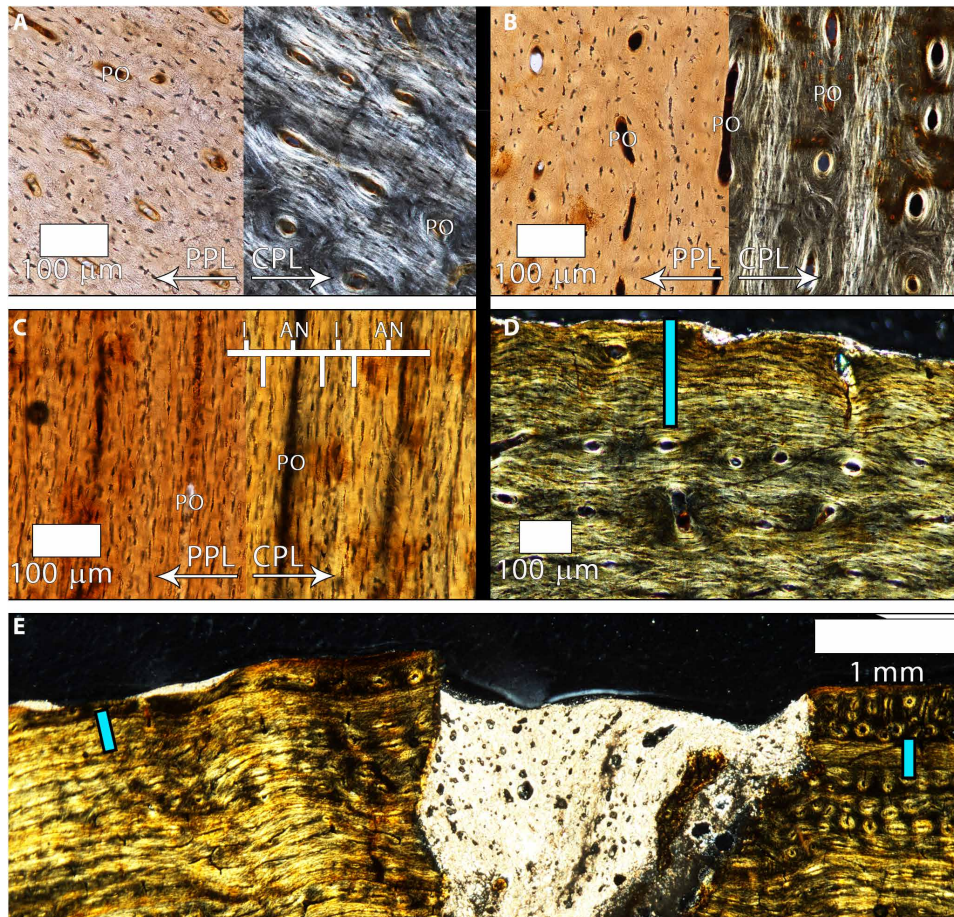


Fig. 1. Femur histology of tyrannosaurid specimens BMRP 2002.4.1 and BMRP 2006.4.4. (A) Mid-cortex of the transverse thin section of BMRP 2002.4.1. Plane-polarized light (PPL) emphasizes osteocyte lacuna density and variability in shape within the laminae, as well as longitudinal primary osteons. In CPL, there is a weak preferred fiber arrangement parallel to the transverse plane of section reflected by regional birefringence. Many primary osteons (POs) have uniformly isotropic fibers with rounded osteocyte lacunae. (B) Mid-cortex of the transverse thin section of BMRP 2006.4.4. Osteocyte lacuna density and variability in shape within the laminae are evident in PPL. CPL reveals varying birefringence associated with bone fiber orientation, but there is a weak preferred fiber arrangement parallel to the transverse plane of section reflected by regional birefringence. Many POs are composed of uniformly isotropic fibers with rounded osteocyte lacunae. (C) Longitudinal section of the mid-cortex of BMRP 2006.4.4. Vascular canals appear as near-vertical, thin, dark columns. As in the transverse section, the primary laminae between POs contain variably arranged osteocyte lacunae. In CPL, the laminae are weakly isotropic (I), corresponding to the poorly organized parallel orientation of fibers in the transverse plane. The laterally compressed osteocyte lacunae in POs are embedded within a uniformly birefringent [anisotropic (AN)] matrix in CPL, indicating that the PO lamellae are longitudinally oriented parallel-fibered bone (LP). (D) On the posteromedial side of the transverse section of BMRP 2006.4.4, there is a parallel-fibered annulus located at the periosteal surface (thickness indicated with blue line). Photographed in CPL. (E) In the transverse section on the posterolateral side, the annulus shown in (D) (blue lines) is overlain by highly isotropic woven-fibered laminae.

In the tibia transverse section of BMRP 2002.4.1 (Fig. 2A and fig. S4), longitudinal primary osteons are isotropic in circularly polarized light (CPL), but fibers of primary osteons encircling laminar, circular, and plexiform vascular canals are anisotropic. In contrast, primary osteons in the tibia of BMRP 2006.4.4 are frequently isotropic regardless of vascular canal orientation. Because of its proximal sampling location, the cortical shape of the tibia from BMRP 2006.4.4 in transverse section differs from that of BMRP 2002.4.1 and incorporates the fibular crest on the lateral side (figs. S2D and S8, A and F). Highly vascularized reticular woven tissue is present on the anterior and anterolateral periosteal surfaces (Fig. 2C). In both individuals, the thickest tibial cortex is located anteriorly.

Of special note, within the medullary cavity of the femur and tibia of BMRP 2006.4.4, isotropic, vascularized, primary tissue is separated

from the cortex by a lamellar endosteal layer. These features are morphologically consistent with medullary bone (11); however, additional studies on the systemic nature of this tissue throughout BMRP 2006.4.4 and biochemical tests on this tissue are necessary to test this hypothesis.

Cyclical growth marks (CGMs), resembling tree rings in transverse thin section, were observed in the femora and tibiae of both BMRP specimens. Studies on extant vertebrates demonstrate that CGMs result from brief interruptions in osteogenesis, occurring with annual periodicity and typically coinciding with the nadir (12). The annual pauses in bone apposition are recorded as CGMs in cortical microstructure as either pronounced lines of arrested growth (LAGs) or diffuse annulus rings. On the basis of counting CGMs, BMRP 2002.4.1 was at least 13 years old at death (13 CGMs in the femur

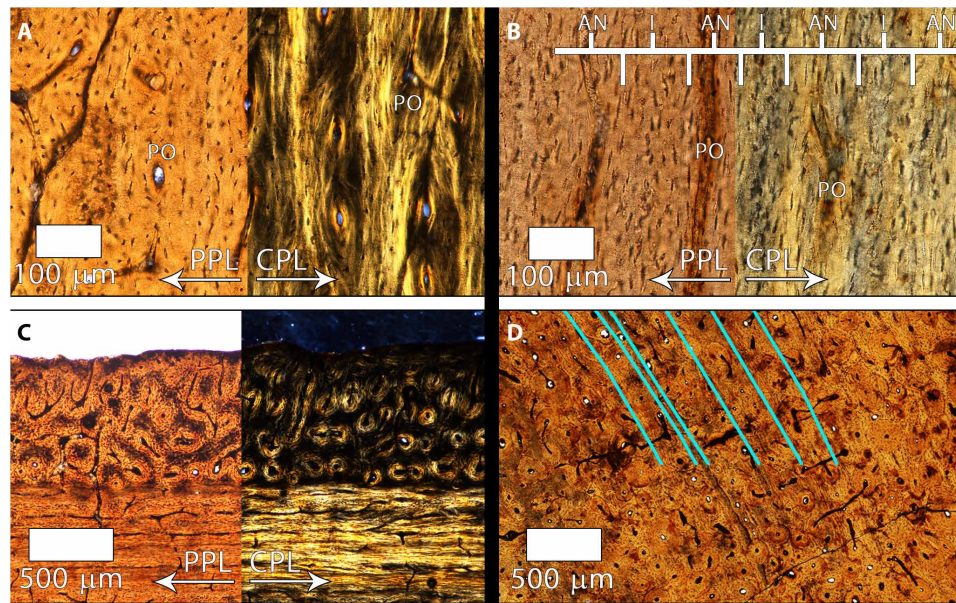


Fig. 2. Tibia histology of tyrannosaurid specimens BMRP 2002.4.1 and BMRP 2006.4.4. (A) Transverse mid-cortex thin section of BMRP 2002.4.1. Longitudinal POs are evident, and PPL emphasizes osteocyte lacuna density and variability in shape within laminae. CPL reveals varying birefringence associated with bone fiber orientation, but with a weak arrangement of fibers parallel to the transverse plane of section. Many POs are composed of highly isotropic fibers with rounded osteocyte lacunae. (B) Longitudinal thin section of the mid-cortex of BMRP 2002.4.1. Vascular canals appear as near-vertical, dark columns. Adjacent to the vascular canals, the POs contain laterally compressed osteocyte lacunae. CPL demonstrates that the laterally compressed osteocyte lacunae of POs are embedded within a uniformly birefringent matrix (anisotropic), indicating that the lamellae of POs are LP. Osteocyte lacunae orientation varies in the thin laminae between POs. In CPL, the laminae are weakly isotropic, corresponding to the weak arrangement of parallel fibers in transverse section. (C) In transverse thin section, the periosteal surface of BMRP 2006.4.4 on the anterior side consists of reticular POs within laminae of highly isotropic, woven tissue. (D) Within the anterior and anteromedial innermost cortex of BMRP 2006.4.4, in transverse thin section, six closely spaced LAGs are visible interstitially. Blue lines highlight the LAG trajectories.

and 10 CGMs in the tibia), and BMRP 2006.4.4 was at least 15 years old at death (15 CGMs in the femur and 13 to 18 CGMs in the tibia). Typically, vertebrate long bone cortices will exhibit widely spaced CGMs within the cortex when young, corresponding to high annual osteogenesis. In subadults, CGMs become more closely spaced as osteogenesis decreases approaching adult size [e.g., (10)]. In contrast to these frequently observed patterns, the spacing of CGMs was unexpectedly variable throughout the femur and tibia cortices of both BMRP specimens.

In the femur of BMRP 2006.4.4, there is an annulus at the periosteal surface on the medial side (Fig. 1D), but when followed posteriorly, the annulus is within the outer cortex, while fibrolamellar tissue makes up the cortex of the periosteal surface (Fig. 1E). Within the innermost cortex on the anterolateral side, six LAGs are closely spaced (Fig. 2D). Because of resorption from the medullary drift, these LAGs are absent within the innermost cortex of the posterior and lateral sides.

Prondvai *et al.* (13) demonstrated that inaccurate bone microstructure interpretations are possible if the mineralized tissue is observed in only a single plane; specifically, the more slowly formed parallel-fibered mineral arrangement could be mistaken for the rapidly deposited woven-fibered mineral arrangement, which has direct bearing on growth rate interpretations. Therefore, the femur of BMRP 2006.4.4 was longitudinally sectioned in an anterolateral-posteromedial plane, and the tibia of BMRP 2002.4.1 was sectioned in a medial-lateral plane to accurately assess tissue organization and associated relative growth rates (Figs. 1C and 2B, and figs. S2, B and C, S5, and S7). In the femur of BMRP 2006.4.4, vascular canals are arranged parallel

to the plane of section and to the shaft of the long bone. Adjacent to the vascular canals, bone fibers are highly anisotropic in CPL and contain osteocyte lacunae with long axes arranged parallel to the vascular canals and plane of section. Tissue of the laminae between primary osteons varies locally in degree of isotropy, with corresponding variable shape in osteocyte lacunae. On the medial side of the longitudinal section through the tibia of BMRP 2002.4.1, vascular canals are arranged obliquely with numerous communications (fig. S5B). From the mid- to the outer cortex, vascular canals are more uniformly parallel to the bone shaft, with fewer transverse Volkmann's canals (fig. S5C). Adjacent to vascular canals, fibers of the primary osteons are anisotropic in CPL with longitudinally flattened osteocyte lacunae. Fibers within the primary laminae vary locally in isotropy and osteocyte lacuna orientation (Fig. 2B). The lateral cortex is thinner than the medial cortex, and vascular canals are more closely spaced with fewer communicating canals (fig. S5D).

DISCUSSION

Limb bones exhibit moderate growth rates and tension loading

Comparison of BMRP 2002.4.1 and BMRP 2006.4.4 bone fiber organization in the transverse and longitudinal sections using CPL confirms that primary tissue is generally poorly organized parallel fibered to weakly woven. Dense osteocyte lacunae and poor bone fiber organization, in combination with a rich vascular network of reticular, laminar, and plexiform primary osteons, are characteristics that empirically correspond to elevated osteogenesis ranging from 5 to

90 $\mu\text{m}/\text{day}$ (10). Nonetheless, the frequency of longitudinal vascularity, as well as regionally prevalent poorly organized parallel fiber bundles within the transverse sections, suggests that annual growth rates were nearer the lower bound (10). The BMRP individuals did, however, experience occasional periods of faster growth indicated by bands of regionally isotropic woven laminae with reticular vascularity (e.g., Figs. 1E and 2C, and figs. S6D and S8, C and D) (10).

In both BMRP specimens, the majority of primary osteons as well as some secondary osteons were isotropic in the transverse section. Corresponding anisotropy in longitudinal examination confirms that the fiber bundles within osteons are longitudinally arranged (Figs. 1C and 2B, and fig. S5, B to D). Studies on long bone response to loading show that longitudinal collagen fiber orientation within secondary osteons is commonly found in habitually tension-loaded regions (14), which may also apply to primary osteon collagen fiber orientation. As such, future studies on tyrannosaurid locomotion biomechanics may benefit from incorporation of osteohistology.

Relative skeletal maturity

Rather than exhibiting an external fundamental system (EFS) (Fig. 3), a woven-parallel complex extends to the periosteal surface in both tyrannosaurid specimens. Thus, histology supports morphological observations that BMRP 2002.4.1 and BMRP 2006.4.4 were skeletally immature individuals at death (10). In lieu of epiphyseal fusion, which most reptile taxa lack, an EFS is the only way to conclusively confirm attainment of asymptotic adult body length from the long bones of a vertebrate. When present, the EFS occupies the periosteal surface as either closely spaced LAGs (separated by micrometers) (Fig. 3A) or as a thick, primarily avascular annulus (Fig. 3B) (10). CGMs close to the periosteal surface can sometimes be mistaken for an EFS. In the case of BMRP 2006.4.4, an annulus is present at the periosteal surface of both the femur (Fig. 1D) and tibia (fig. S8E), but when the annulus is followed around the cortex, in both cases it becomes embedded within the outer cortex and superseded by woven primary tissue (Figs. 1E and 2C). The proximity of the annulus to the periosteal surface instead suggests that BMRP 2006.4.4 died soon after growth resumed following the annual hiatus and that cortical osteogenesis was directional.

Ontogenetic age

On the basis of femur CGM count, BMRP 2002.4.1 was >13 years old at death, which is 2 years older than the original estimate by Erickson (8) based on fibula CGM count. The slightly larger BMRP 2006.4.4 was >15 years old. The number of CGMs missing due to medullary expansion is unknown, precluding an exact age at death for BMRP 2002.4.1 and BMRP 2006.4.4. Although the number of missing CGMs could be predicted on the basis of innermost zonal thicknesses and a process of retrocalculation [e.g., (5, 10)], the variable spacing between CGMs observed in BMRP 2002.4.1 and BMRP 2006.4.4 and other tyrannosaurs (15) renders the technique unreliable in this case, and it was not attempted.

Within the innermost cortex of BMRP 2006.4.4, there is a tight stacking of six CGMs (Fig. 2D). Because the CGMs remain parallel about the cortex and do not merge, they either represent a single hiatus in which growth repeatedly ceased and resumed (totaling 13 years of growth) or up to 6 years where relatively little growth occurred annually (totaling up to 18 years of growth) (9, 16). This tight stacking of six CGMs is not observed in the femur of BMRP 2006.4.4, which preserves 15 CGMs. The CGM count from the partial tibia of

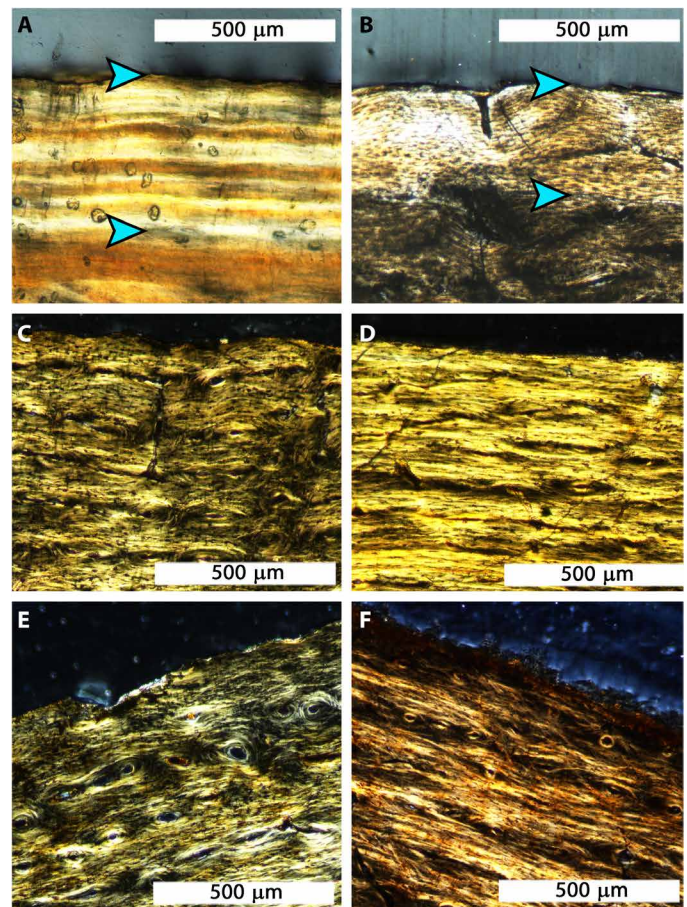


Fig. 3. The presence of an EFS at the periosteal surface of a long bone indicates skeletal maturity, while the absence of an EFS indicates that the bone is still growing at the time of death. (A) An EFS composed of tightly stacked birefringent LAGs (between blue arrowheads) at the periosteal surface of an *Alligator mississippiensis*. **(B)** The EFS (between blue arrowheads) in an ostrich (*Struthio camelus*) is made of nearly avascular, birefringent parallel-fibered to lamellar primary tissue. **(C)** No EFS is present at the periosteal surface of the femur of BMRP 2002.4.1, **(D)** the tibia of BMRP 2002.4.1, **(E)** the femur of BMRP 2006.4.4, or **(F)** the tibia of BMRP 2006.4.4. All panels are shown in transverse thin section, with CPL.

BMRP 2006.4.4 is questionable because the proximal sampling location away from midshaft incorporates the fibular crest, introducing associated regions of remodeling and directional growth affecting apposition interpretations. Because of this and their absence in the femur, the observed grouping of six CGMs is conservatively interpreted as a single hiatus event. Similar instances of a single hiatus represented by narrowly spaced LAGs are reported in other tyrannosaurids (15). If this grouping of CGMs instead represents 6 years of protracted growth, then BMRP 2006.4.4 demonstrates the extent to which these individuals could adjust growth rate based on resource availability, in this case prolonging the ontogenetic duration of BMRP 2006.4.4 as a mid-sized carnivore.

Bone tissue organization was similar across femora and tibiae, suggesting that both bones record annual increases in body size equally well. If the stacked CGMs of BMRP 2006.4.4 reflect a single hiatus, then each femur preserved more CGMs than the associated tibia. Previous studies demonstrated that intraskeletal inconsistencies in

CGM counts are due to variable rates of medullary cavity expansion or cortical drift across elements (9, 17, 18) when sampled at midshaft. Therefore, our preliminary assessment of *T. rex* intraskeletal histology suggests that the femur is more informative than the tibia, despite regions of cortical remodeling from tendinous entheses about the cortex. Additional intraskeletal histoanalyses of tyrannosaurid specimens are necessary to test whether the femur is the preferred weight-bearing bone for simultaneous assessments of annual growth rates and skeletochronology.

In addition to ontogenetic zonal thickness variability within the cortex, zonal thickness also changed with respect to cortical orientation. That is, zones were often much thinner relative to one another on one side of the transverse section and much thicker on another side (e.g., fig. S4, G and H). This pattern is particularly noticeable in the tibia of BMRP 2002.4.1 (medial cortical zones are thickest) and the femur of BMRP 2006.4.4 (posteromedial cortical zones are thickest). This observation implies that directional cortical growth occurred over ontogeny and stresses the necessity of complete transverse sections for histological analysis: Obtaining a fragment or core for study from one orientation may result in erroneous interpretations of growth rate and skeletal maturity.

Variability in annual growth as a response to resource abundance

Interpretations of relative maturity in nonavian dinosaurs often rely on reported trends in the thickness of cortical zones between CGMs from the inner to the outer cortex (10). Zone thickness is typically greatest within the innermost cortex, corresponding to rapid annual growth early in life. Zones become progressively thinner in the mid- to the outer cortex of older individuals, as annual growth rate decreases approaching asymptotic body length. These general trends provide the interpretive foundation for the two previous histology-based ontogenetic studies on *Tyrannosaurus* growth (4, 5). The spacing of CGMs within the outer cortices of BMRP 2002.4.1 and BMRP 2006.4.4 (Fig. 4) is narrower than between some CGMs deeper within the cortices, which suggests that, although not adults, the specimens were approaching a body length asymptote at about one-half the body length of FMNH PR 2081. However, annual zonal thicknesses between CGMs deeper within the cortices of BMRP 2002.4.1 (Fig. 4A) and BMRP 2006.4.4 (Fig. 4B) are variable, and zones do not consistently progress from widely spaced within the inner cortex to more closely spaced in the outer cortex. Because of unpredictable spacing within the cortex, reduced zonal thickness near the periosteal surface is likely an unreliable indicator of skeletal maturity in BMRP 2002.4.1 and BMRP 2006.4.4. Variable zonal thicknesses are, thus, likely to be observed in ontogenetically older *T. rex* individuals. To test this hypothesis, we examined femur and tibia thin sections from *T. rex* specimens USNM PAL (National Museum of Natural History) 555000, MOR (Museum of the Rockies) 1125, MOR 1128, MOR 1198, and CCM (Carter County Museum) V33.1.15. In all individuals, variability in annual zonal thicknesses was observed. In particular, compared to zone spacing within the mid-cortex, noticeably thinner zones are present within the innermost cortex of USNM PAL 555000 (Fig. 4C) and MOR 1128 (Fig. 4D). These results contradict the mathematically predictable zonal spacing in *T. rex* long bones reported by Horner and Padian (5), which used some of the same specimens reassessed in the present study. Results further suggest not only that BMRP 2002.4.1 and BMRP 2006.4.4 had not yet entered the accelerated growth period proposed for this

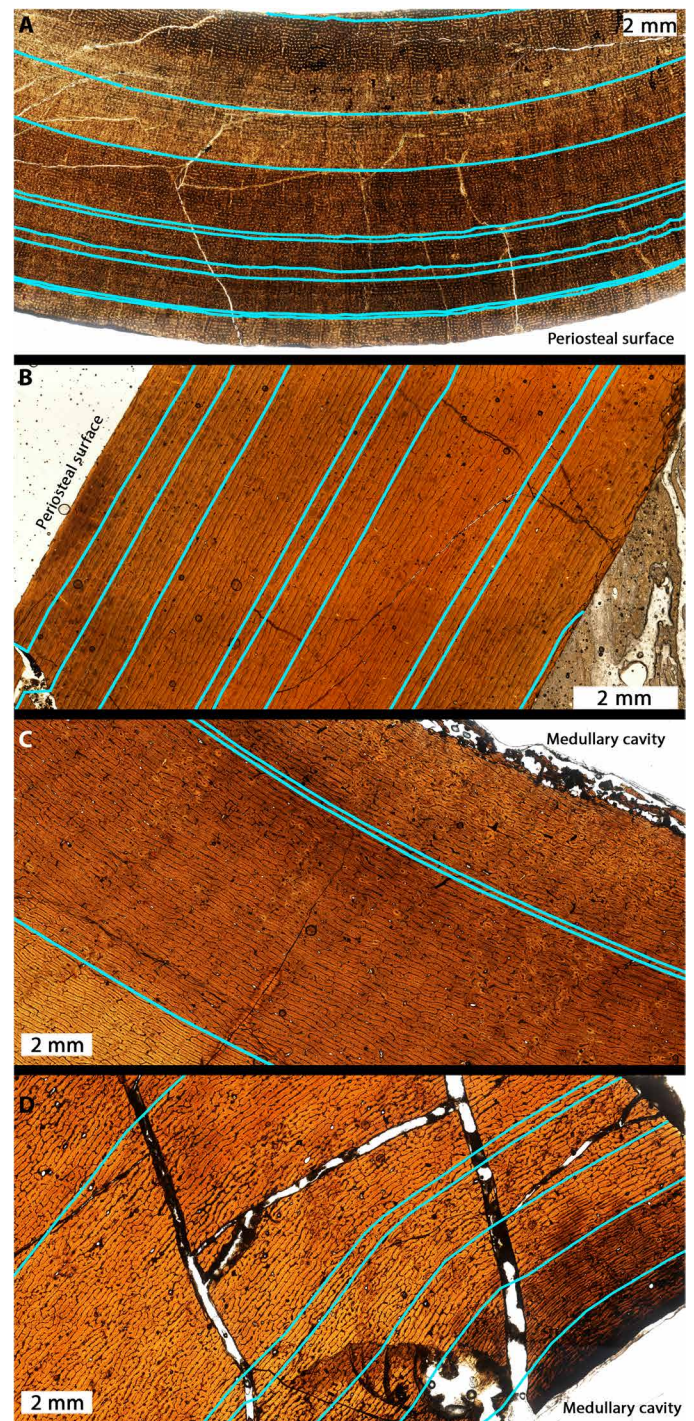


Fig. 4. Examples of variable CGM (blue lines) spacing in tyrannosaurids examined for this study. (A) The variability of CGM spacing in the femur of BMRP 2002.4.1 and (B) the tibia of BMRP 2006.4.4 may imply that these individuals were approaching asymptotic body length. However, CGMs within the innermost cortices of much larger *T. rex* specimens (C) USNM PAL 555000 and (D) MOR 1128 demonstrate that the CGM spacing is not a reliable indicator of relative maturity status. All panels are shown in transverse thin section.

taxon (4, 5) but also that the accuracy of the generalized *T. rex* body mass curve from Erickson *et al.* (4) would be affected by undetected individual variation in annual growth.

Variable LAG spacing is reported in ornithomimids, ornithopods [(19) and references therein], and other tyrannosauroids (15) and may correlate with annual resource abundance (12, 19). Our data suggest that this trait also characterizes *T. rex*: Because the level of bone tissue organization within zones remained the same from the innermost cortex to the periosteal surface in the BMRP specimens, growth rates were within a similar range from year to year. To produce these extremes in annual bone apposition, the duration of the growth hiatus must have varied annually. On the basis of the larger *T. rex* specimens examined here for comparison, the adjustment of annual growth hiatus duration in response to resource abundance is a physiological characteristic observed throughout *T. rex* ontogeny. Regardless of cause, unpredictable CGM spacing observed here and in previous studies stresses caution when inferring relative maturity based on cortical LAG spacing (19). The observation of closely spaced CGMs within the innermost cortices of larger *T. rex* validates our interpretation that the thin zonal spacing observed in the outermost cortices of BMRP 2002.4.1 and BMRP 2006.4.4 are not reliable indicators of relative maturity when an EFS is absent.

Implications for the *Nanotyrannus* hypothesis

The bone microstructural interpretations discussed here not only provide insight into *T. rex* ontogeny but also have bearing on discussions concerning CMNH (Cleveland Museum of Natural History) 7541 and *Nanotyrannus*. CMNH 7541 consists of a small isolated skull 572 mm in length (20). Inferred to be sympatric with *T. rex*, it was originally named *Gorgosaurus lancensis* (21). In 1988, Bakker *et al.* (22) redescribed CMNH 7541 as an adult specimen of a new genus, *Nanotyrannus*. Using an extensive empirical dataset, Carr and Williamson (23) formally synonymized *Nanotyrannus* into *Tyrannosaurus* in 2004, supporting the interpretation of CMNH 7541 as a juvenile *T. rex* proposed by Rozhdestvensky in 1965 (24). Presently, most tyrannosaurid specialists consider CMNH 7541 and possible referred specimens to be juvenile *T. rex* based on morphological skull features shared with those found in undisputed juvenile individuals of other tyrannosaurid taxa [e.g., (2, 20, 23, 25–28)]. Nonetheless, several publications have since argued for the validity of *Nanotyrannus* based not only on morphological characters of the CMNH 7541 type skull but also on characters from the somewhat larger skull of BMRP 2002.4.1 (720 mm in length) [e.g., (29–33)], which some researchers have assigned to *Nanotyrannus* based on shared morphological characters they consider adult autapomorphies of the taxon [e.g., (29–33)]. Currently, BMRP 2002.4.1 is the only accessioned specimen with postcranial skeletal elements preserved that is specifically argued by proponents of *Nanotyrannus* as belonging to that genus [e.g., (29–32)]. Because CMNH 7541 lacks the postcranial skeleton and proponents of *Nanotyrannus* refer BMRP 2002.4.1 to that taxon, the limb bone histology of BMRP 2002.4.1 (and additionally BMRP 2006.4.4; see the Supplementary Materials for taxonomic discussion) reveals the life history of CMNH 7541 by proxy.

Here, we provide histological data that can be used to reject the hypothesis that *Nanotyrannus* was erected on the basis of a skeletally mature “pygmy” individual, resulting in two remaining alternative hypotheses: (i) *Nanotyrannus* is a valid taxon, but the holotype and all currently referred specimens including BMRP 2002.4.1 and BMRP 2006.4.4 are immature, with no skeletally mature individuals yet known; and (ii) CMNH 7541, BMRP 2002.4.1, BMRP 2006.4.4, and other mid-sized tyrannosaurid specimens collected from the HCF represent juvenile ontogenetic stages of *T. rex*. Thus far, the femur and tibia of BMRP 2002.4.1 and BMRP 2006.4.4 are the only weight-

bearing bones of Upper Cretaceous HCF tyrannosaurids described histologically from complete transverse sections, and these universally demonstrate features characteristic of actively growing juvenile dinosaurs that had not yet entered an exponential phase of growth (as demonstrated by our new data identifying noticeably thinner zones within the innermost cortex of large-bodied *T. rex* specimens such as USNM PAL 55500). On the basis of these data, the latter hypothesis is most parsimonious and is congruent with the morphology-based conclusions of Carr (20) and Carr and Williamson (23). Incorporating additional mid-sized HCF tyrannosaurid specimens into this histology-based relative maturity assessment is necessary to further support or refute the parsimonious hypothesis.

Paleoecological implications

Synonymization of *Nanotyrannus* with *T. rex* means that rather than two sympatric tyrannosaurid taxa within faunal assemblages of the HCF, only one valid tyrannosaur species—*T. rex*—is currently recognized. As an adult, *T. rex* occupied the large-sized carnivore niche in the latest Cretaceous HCF ecosystem (2, 34), achieving an average adult body mass of ~9502 kg (6) by 20 years of age (4). BMRP 2002.4.1 and BMRP 2006.4.4, at >13 and >15 years of age, respectively, were only half the length of an adult *T. rex* (6, 7). Hutchinson *et al.* (6) obtained an averaged body mass estimate of 954 kg for BMRP 2002.4.1, which falls within the mid-sized dinosaur body mass range defined by Holtz (35) as 50 to 1000 kg. Our histological confirmation of BMRP 2002.4.1 and BMRP 2006.4.4 as mid-sized juveniles is therefore congruent with a hypothesized delayed onset of exponential growth in *T. rex* relative to the ontogenetic timing of exponential growth in other tyrannosaurids (4). Because *T. rex* attained its great size late in ontogeny (4), many aspects of its biology likely differed between juvenile and adult individuals, leading to hypotheses that it used ontogenetic niche partitioning (2, 36, 37), where prey size is a function of body size (2, 36, 38). This feeding strategy is observed today in the extant archosaur *Alligator*, because it occupies different carnivore niches before and after achieving skeletal maturity (39). Most recently, Peterson and Daus (40) demonstrated that although able to puncture bone, late-stage juvenile *T. rex* could not yet crush bone or engage in osteophagy, and therefore engaged in a feeding strategy distinct from adults.

Our histological assessment of BMRP 2002.4.1 and BMRP 2006.4.4 provides data critical to understanding juvenile *T. rex* biology and ecology, and additional evidence that there were no sympatric tyrannosaurids in the HCF. Furthermore, we hypothesize that ontogenetic niche partitioning, coupled with an ability to adjust annual growth hiatus duration to track resource abundance, made *T. rex* one of the most successful nonavian theropods.

MATERIALS AND METHODS

BMRP 2002.4.1 and BMRP 2006.4.4 were collected from the HCF of Carter County, Montana. The specimen BMRP 2002.4.1 consists of a nearly complete skull with associated postcrania, including a partial femur [estimated length, 68.8 cm; (7)] and complete tibiae. BMRP 2006.4.4 is far less complete and lacks cranial material, but with a femur length of 77.4 cm, it is slightly larger (and presumably ontogenetically older) than BMRP 2002.4.1.

Histological analysis

The partial femur of BMRP 2002.4.1 and the partial tibia of BMRP 2006.4.4 were histologically processed by the MOR for an earlier

project, and the resulting thin section slides were made available on loan to the senior author. Additional thin sections were produced for the current study to directly compare histological features across bones of BMRP 2002.4.1 and BMRP 2006.4.4: Full transverse thin sections from the femur of BMRP 2006.4.4 and the tibia of BMRP 2002.4.1 were produced following the methodology of Padian and Lamm (10) with the permission of BMRP and the Bureau of Land Management.

Fibula thin section slides of BMRP 2002.4.1 and BMRP 2006.4.4 were earlier produced for separate projects. An ontogenetic age of 11 for BMRP 2002.4.1 was published by Erickson (8) based on fibula histology, and an ontogenetic age of BMRP 2006.4.4 was not published. Access to the aforementioned fibula thin sections for comparative histology and skeletochronology in this study was denied.

As summarized by Prondvai *et al.* (13), modern bone is composed of integrated hydroxyapatite crystals and collagen fibrils, with long axes arranged in parallel. Thus, the orientation of inorganic hydroxyapatite minerals implies collagen fiber arrangement in fossil bone, and this orientation can be inferred visually by the intensity of birefringence associated with anisotropy in polarized light: If the fiber bundles are cut across their longitudinal axis, they will appear bright (anisotropic), whereas if cut transversely, they will remain dark (isotropic). Bone fiber orientation is typically diagnosed from a thin section of bone cut transverse to the long axis of a diaphysis. Bone tissue was classified as parallel fibered or lamellar if uniformly anisotropic with flattened osteocyte lacunae (i.e., lacuna long axis parallel to fiber orientation) and woven if uniformly isotropic with rounded lacunae. Without examining bone tissue in the longitudinal as well as transverse planes, it is impossible to distinguish woven tissue, which should remain isotropic in both orientations, from longitudinally oriented parallel-fibered or lamellar tissue, which is isotropic in the transverse section and can therefore be mistaken for woven tissue. This distinction is critical, because ranges of daily apposition rates are frequently assigned on the basis of fiber orientation [see (13) for discussion]. For this reason, when thin sections were produced for this study, each specimen was sectioned both longitudinally and transversely to more accurately assess bone fiber orientation.

Full transverse sections from the femoral and tibial diaphyses of BMRP 2002.4.1 and BMRP 2006.4.4 were removed from the bones using a circular saw with a continuous rim diamond blade. The samples removed were molded and cast, and the cast replicas were restored to the fossil bones. The samples removed were then embedded in Silmar polyester resin, and transverse wafers were cut (~3 to 4 mm thick) to either side of the line of minimum circumference with a circular saw and continuous rim diamond blade. These wafers were glued to frosted glass slides and polished on a variable speed grinder to mirror finish using a series of 60, 120, 180, 320, 600, 800, and 1200 silicon carbide grit papers and 5- and 1- μ m hand-polish slurries. Final slide thicknesses were between 97 and 177 μ m. Longitudinal sections were made from the embedded diaphysis samples, along a lateral-medial plane in the tibia of BMRP 2002.4.1 and an anterolateral-posteromedial plane in the femur of BMRP 2006.4.4, capturing the thickest regions of cortex.

Thin sections were analyzed using a Nikon Eclipse Ni-U polarizing microscope and plane-polarized light (i.e., only the polarizer in position), CPL, and cross-polarized light with 540-nm lambda filter. Photomicrographs were taken using a Nikon Fi2 microscope camera. Composite images of each full thin section at $\times 20$ total magnification were obtained through the use of an automated Applied Scien-

tific Instrumentation microscope stage and Nikon Elements: Documentation software. Annually formed CGMs, including LAGs and annuli, were identified and digitally traced using Adobe Photoshop CC. Comparisons of annual zonal thicknesses between CGMs were made along a transect, and measurements were taken in Adobe Photoshop CC. Histological descriptions were made from observations using CPL and follow the terminology of Padian and Lamm (10) and Prondvai *et al.* (13). A CGM was identified as an annulus if it consisted of a diffuse band of parallel-fibered bone and interpreted as a period of considerably decreased osteogenesis. A LAG was identified as a thin hypermineralized ring, indicating a period when osteogenesis ceased altogether.

SUPPLEMENTARY MATERIALS

Supplementary material for this article is available at <http://advances.sciencemag.org/cgi/content/full/6/1/eaax6250/DC1>

Supplementary Materials and Methods

Fig. S1. Hind limb elements of BMRP 2006.4.4.

Fig. S2. Femur and tibia histology overview of tyrannosaurid specimens BMRP 2002.4.1 and BMRP 2006.4.4.

Fig. S3. Fragmentary femur transverse thin section of BMRP 2002.4.1.

Fig. S4. Transverse thin section histology of the right tibia of BMRP 2002.4.1.

Fig. S5. Longitudinal thin section of BMRP 2002.4.1 tibia.

Fig. S6. Transverse and longitudinal thin sections were produced from the left femur of BMRP 2006.4.4.

Fig. S7. Longitudinal thin section of the left femur from BMRP 2006.4.4.

Fig. S8. Transverse thin section of the left tibia of BMRP 2006.4.4.

References (15, 41–54)

[View/request a protocol for this paper from Bio-protocol.](#)

REFERENCES AND NOTES

- H. F. Osborn, *Tyrannosaurus* and other Cretaceous carnivorous dinosaurs. *Bull. Am. Mus. Nat. Hist.* **21**, 259–265 (1905).
- S. L. Brusatte, M. A. Norell, T. D. Carr, G. M. Erickson, J. R. Hutchinson, A. M. Balanoff, G. S. Bever, J. N. Choiniere, P. J. Makovicky, X. Xu, Tyrannosaur paleobiology: New research on ancient exemplar organisms. *Science* **329**, 1481–1485 (2010).
- P. L. Larson, K. Carpenter, *Tyrannosaurus Rex, the Tyrant King*. (Indiana Univ. Press, Bloomington, 2008).
- G. M. Erickson, P. J. Makovicky, P. J. Currie, M. A. Norell, S. A. Yerby, C. A. Brochu, Gigantism and comparative life-history parameters of tyrannosaurid dinosaurs. *Nature* **430**, 772–775 (2004).
- J. R. Horner, K. Padian, Age and growth dynamics of *Tyrannosaurus rex*. *Proc. R. Soc. Lond. B Biol. Sci.* **271**, 1875–1880 (2004).
- J. R. Hutchinson, K. T. Bates, J. Molnar, V. Allen, P. J. Makovicky, A computational analysis of limb and body dimensions in *Tyrannosaurus rex* with implications for locomotion, ontogeny, and growth. *PLOS ONE* **6**, e26037 (2011).
- P. J. Currie, Allometric growth in tyrannosaurids (Dinosauria: Theropoda) from the Upper Cretaceous of North America and Asia. *Can. J. Earth Sci.* **40**, 651–665 (2003).
- G. M. Erickson, Assessing dinosaur growth patterns: A microscopic revolution. *Trends Ecol. Evol.* **20**, 677–684 (2005).
- H. N. Woodward, J. R. Horner, J. O. Farlow, Quantification of intraskeletal histovariability in *Alligator mississippiensis* and implications for vertebrate osteohistology. *PeerJ* **2**, e422 (2014).
- K. Padian, E.-T. Lamm, *Bone Histology of Fossil Tetrapods: Advancing Methods, Analysis, and Interpretation* (University of California Press, Berkeley, 2013), p. 285.
- M. H. Schweitzer, W. Zheng, L. Zanno, S. Werning, T. Sugiyama, Chemistry supports the identification of gender-specific reproductive tissue in *Tyrannosaurus rex*. *Sci. Rep.* **6**, 23099 (2016).
- M. Köhler, N. Marin-Moratalla, X. Jordana, R. Aanes, Seasonal bone growth and physiology in endotherms shed light on dinosaur physiology. *Nature* **487**, 358–361 (2012).
- E. Prondvai, K. H. W. Stein, A. de Ricqlès, J. Cubo, Development-based revision of bone tissue classification: the importance of semantics for science. *Biol. J. Linn. Soc.* **112**, 799–816 (2014).
- J. G. Skedros, S. D. Mendenhall, C. J. Kiser, H. Winet, Interpreting cortical bone adaptation and load history by quantifying osteon morphotypes in circularly polarized light images. *Bone* **44**, 392–403 (2009).

15. L. E. Zanno, R. T. Tucker, A. Canoville, H. M. Avrahami, T. A. Gates, P. J. Makovicky, Diminutive fleet-footed tyrannosaurid narrows the 70-million-year gap in the North American fossil record. *Commun. Biol.* **2**, 64 (2019).
16. M. H. Caetano, J. Castanet, Variability and microevolutionary patterns in *Triturus marmoratus* from Portugal: age, size, longevity and individual growth. *Amphibia Reptilia* **14**, 117–129 (1993).
17. I. Griffiths, Skeletal lamellae as an index of age in Heterothermous Tetrapods. *Ann. Mag. Nat. Hist.* **4**, 449–465 (1961).
18. J. M. Hutton, Age determination of living Nile crocodiles from the cortical stratification of bone. *Copeia* **2**, 332–341 (1986).
19. T. M. Cullen, D. C. Evans, M. J. Ryan, P. J. Currie, Y. Kobayashi, Osteohistological variation in growth marks and osteocyte lacunar density in a theropod dinosaur (Coelurosauria: Ornithomimidae). *BMC Evol. Biol.* **14**, 231 (2014).
20. T. D. Carr, Craniofacial ontogeny in Tyrannosauridae (Dinosauria, Coelurosauria). *J. Vertebr. Paleontol.* **19**, 497–520 (1999).
21. C. W. Gilmore, New carnivorous dinosaur from the Lance formation of Montana. *Smithson. misc. collect.* **106**, 1–19 (1946).
22. R. T. Bakker, M. Williams, P. J. Currie, *Nanotyrannus*, a new genus of pygmy tyrannosaur, from the latest Cretaceous of Montana. *Hunteria* **1**, 1–30 (1988).
23. T. D. Carr, T. E. Williamson, Diversity of Late Maastrichtian Tyrannosauridae (Dinosauria: Theropoda) from western North America. *Zool. J. Linnean Soc.* **142**, 419–523 (2004).
24. A. K. Rozhdestvensky, Growth changes in Asian dinosaurs and some problems of their taxonomy. *Paleontol. Zh.* **3**, 95–109 (1965).
25. C. A. Brochu, Osteology of *Tyrannosaurus rex*: Insights from a nearly complete skeleton and high-resolution computed tomographic analysis of the skull. *J. Vertebr. Paleontol. Memoir* **22**, 1–138 (2003).
26. S. L. Brusatte, T. D. Carr, The phylogeny and evolutionary history of tyrannosaurid dinosaurs. *Sci. Rep.* **6**, 20252 (2016).
27. S. L. Brusatte, T. D. Carr, T. E. Williamson, T. R. Holtz Jr., D. W. E. Hone, S. A. Williams, Dentary groove morphology does not distinguish ‘*Nanotyrannus*’ as a valid taxon of tyrannosaurid dinosaur. Comment on: “Distribution of the dentary groove of theropod dinosaurs: Implications for theropod phylogeny and the validity of the genus *Nanotyrannus* Bakker et al., 1988”. *Cretac. Res.* **65**, 232–237 (2016).
28. T. R. Holtz Jr., *The Dinosauria*, D. Weishampel, P. Dodson, H. Osmolska, Eds. (University of California Press, Berkeley, 2004), pp. 111–136.
29. T. Tsuihiji, M. Watabe, K. Tsogtbaatar, T. Tsubamoto, R. Barsbold, S. Suzuki, A. H. Lee, R. C. Ridgely, Y. Kawahara, L. M. Witmer, Cranial osteology of a juvenile specimen of *Tarbosaurus bataar* from the Nemegt Formation (Upper Cretaceous) of Bugin Tsav, Mongolia. *J. Vertebr. Paleontol.* **31**, 497–517 (2011).
30. J. Schmerge, B. M. Rothschild, Distribution of the dentary groove of theropod dinosaurs: Implications for theropod phylogeny and the validity of the genus *Nanotyrannus* Bakker et al., 1988. *Cretac. Res.* **61**, 26–33 (2016).
31. P. Larson, in *Tyrannosaurid Paleobiology*, M. J. Parrish, R. E. Molnar, P. J. Currie, E. B. Koppelhus, Eds. (Indiana Univ. Press, 2013), chap. 2, pp. 15–53.
32. N. L. Larson, in *Tyrannosaurus rex, the Tyrant King*, P. Larson, K. Carpenter, Eds. (Indiana Univ. Press, Bloomington, 2008), pp. 1–56.
33. L. M. Witmer, R. C. Ridgely, The Cleveland tyrannosaur skull (*Nanotyrannus* or *Tyrannosaurus*): new findings based on CT scanning, with special reference to the braincase. *Kirtlandia* **57**, 61–81 (2010).
34. J. R. Horner, M. B. Goodwin, N. Myhrvold, Dinosaur census reveals abundant *Tyrannosaurus* and rare ontogenetic stages in the Upper Cretaceous Hell Creek Formation (Maastrichtian), Montana, USA. *PLOS ONE* **6**, e16574 (2011).
35. T. R. Holtz Jr., Taxonomic diversity, morphological disparity, and guild structure in theropod carnivore communities: implications for paleoecology and life history strategies in tyrant dinosaurs. *J. Vertebr. Paleontol.* **24**, 72A (2004).
36. T. R. Holtz Jr., *Tyrannosaurus rex, the Tyrant King*, P. Larson, K. Carpenter, Eds. (Indiana Univ. Press, Bloomington, 2008), chap. 20, pp. 371–396.
37. A. Kane, K. Healy, G. D. Ruxton, A. L. Jackson, Body size as a driver of scavenging in theropod dinosaurs. *Am. Nat.* **187**, 706–716 (2016).
38. D. A. Russell, Tyrannosaurs from the Late Cretaceous of western Canada. *National Museum of Natural Sciences, Publications, in Paleontology* **1**, 1–34 (1970).
39. P. Dodson, Functional and ecological significance of relative growth in Alligator. *J. Zool.* **175**, 315–355 (1975).
40. J. E. Peterson, K. N. Daus, Feeding traces attributable to juvenile *Tyrannosaurus rex* offer insight into ontogenetic dietary trends. *PeerJ* **7**, e6573 (2019).
41. B. Brown, The Hell Creek Beds of the Upper Cretaceous of Montana: Their relation to contiguous deposits, with faunal and floral lists and a discussion of their correlation. *Bull. Am. Mus. Nat. Hist.* **23**, 823–845 (1907).
42. J. H. Hartman, K. R. Johnson, D. J. Nichols, *The Hell Creek Formation and the Cretaceous-Tertiary boundary in the northern Great Plains: an integrated continental record of the end of the Cretaceous* (Geological Society of America, 2002), vol. 361.
43. G. P. Wilson, W. A. Clemens, J. R. Horner, J. H. Hartman, *Through the end of the Cretaceous in the type locality of the Hell Creek Formation in Montana and adjacent areas* (Geological Society of America, 2014), vol. 503.
44. G. P. Wilson, Mammalian extinction, survival, and recovery dynamics across the Cretaceous-Paleogene boundary in northeastern Montana, USA. *Geol. Soc. Am.* **503**, 365–392 (2014).
45. C. J. Sprain, P. R. Renne, W. A. Clemens, G. P. Wilson, Calibration of chron C29r: New high-precision geochronologic and paleomagnetic constraints from the Hell Creek region, Montana. *Geol. Soc. Am. Bull.* **130**, 1615–1644 (2018).
46. K. R. Johnson, J. N. Douglas, J. H. Hartman, Hell Creek Formation: A 2001 synthesis. *Geol. Soc. Spec.* **361**, 503–510 (2002).
47. E. C. Murphy, J. W. Hoganson, K. R. Johnson, in *The Hell Creek Formation and the Cretaceous-Tertiary boundary in the northern Great Plains: An Integrated continental record of the end of the Cretaceous*, J. H. Hartman, K. R. Johnson, D. J. Nichols, Eds. (Geological Society of America, 2002), vol. 361, pp. 9–34.
48. E. S. Belt, J. F. Hicks, D. A. Murphy, A pre-Lancian regional unconformity and its relationship to Hell Creek paleogeography in south-eastern Montana. *Rocky Mountain Geol.* **31**, 1–26 (1997).
49. D. M. Henderson, W. H. Harrison, in *Tyrannosaurus rex, the Tyrant King*, P. Larson, K. Carpenter, Eds. (Indiana Univ. Press, Bloomington, 2008), pp. 82–90.
50. E. Snively, A. P. Russell, Functional variation of neck muscles and their relation to feeding style in Tyrannosauridae and other large theropod dinosaurs. *Anat. Rec.* **290**, 934–957 (2007).
51. J. E. Peterson, M. D. Henderson, R. P. Scherer, C. P. Vittore, Face biting on a juvenile tyrannosaurid and behavioral implications. *Palaio* **24**, 780–784 (2009).
52. M. A. Loewen, R. B. Irmis, J. J. Sertich, P. J. Currie, S. D. Sampson, Tyrant dinosaur evolution tracks the rise and fall of Late Cretaceous oceans. *PLOS ONE* **8**, e79420 (2013).
53. T. D. Carr, D. J. Varricchio, J. C. Sedlmayr, E. M. Roberts, J. R. Moore, A new tyrannosaur with evidence for anagenesis and crocodile-like facial sensory system. *Sci. Rep.* **7**, 44942 (2017).
54. H. N. Woodward, T. H. Rich, P. Vickers-Rich, The bone microstructure of polar “hypsiphodontid” dinosaurs from Victoria, Australia. *Sci. Rep.* **8**, 1162 (2018).

Acknowledgments: G. Liggett, G. Smith, and D. Milton with the Bureau of Land Management (permits MTM 90904 and MTM 95725) granted excavation permits and histology processing permission for BMRP specimens. D. Carlson, M. Householder, D. Mauro, and J. Peterson conducted fossil preparation of BMRP 2002.4.1 and BMRP 2006.4.4. J. Mathews provided access to BMRP specimens. J. Scannella and A. Atwater (MOR) allowed access to *T. rex* histology thin sections. Ostrich and alligator thin section images are from specimens repositied at MOR. E. Lamm (MOR) produced the tibia thin sections of BMRP 2006.4.4 and the femur thin sections of BMRP 2002.4.1 for a previous study. N. Carroll granted permission to histologically examine CCM V33.1.15. G. Wilson, T. Carr, S. Brusatte, and T. Holtz provided helpful discussions. C. Tuck and B. Harrison discovered BMRP 2002.4.1. D. Breese and A. Breese discovered BMRP 2006.4.4. We are also thankful to M. Henderson, L. Crampton, and S. Moore. **Funding:** Funding was provided by the Myhrvold Family Charitable Fund, Oklahoma State University Center for Health Sciences, J. Brost and B. Brost, S. Landi, C. Vittore, B. Williams and C. Williams, the Institute of Museum and Library Services, Illinois Department of Natural Resources, Rockford Park District, and Windway Foundation. **Author contributions:** H.N.W., K.T., N.M., and J.R.H. conceived the study. H.N.W. developed the histology procedures and histologically processed the specimens. H.N.W., K.T., and J.R.H. analyzed and interpreted the thin sections. S.A.W. provided the geologic interpretation. L.E.Z. conducted and wrote the taxonomic assessment of BMRP 2006.4.4. H.N.W. wrote the manuscript, with contributions from all other authors. **Competing interests:** Funding for this project in part came from the Myhrvold Family Charitable Fund, founded by N.M. The authors declare that they have no other competing interests. **Data and materials availability:** All data needed to evaluate the conclusions in the paper are present in the paper and/or the Supplementary Materials. Additional data related to this paper, including high-resolution images of manuscript and supplementary figures, may be requested from the authors.

Submitted 8 April 2019

Accepted 1 November 2019

Published 1 January 2020

10.1126/sciadv.aax6250

Citation: H. N. Woodward, K. Tremaine, S. A. Williams, L. E. Zanno, J. R. Horner, N. Myhrvold, Growing up *Tyrannosaurus rex*: Osteohistology refutes the pygmy “*Nanotyrannus*” and supports ontogenetic niche partitioning in juvenile *Tyrannosaurus*. *Sci. Adv.* **6**, eaax6250 (2020).

Growing up *Tyrannosaurus rex*: Osteohistology refutes the pygmy "*Nanotyrannus*" and supports ontogenetic niche partitioning in juvenile *Tyrannosaurus*

Holly N. Woodward, Katie Tremaine, Scott A. Williams, Lindsay E. Zanno, John R. Horner and Nathan Myhrvold

Sci Adv 6 (1), eaax6250.
DOI: 10.1126/sciadv.aax6250

ARTICLE TOOLS <http://advances.sciencemag.org/content/6/1/eaax6250>

SUPPLEMENTARY MATERIALS <http://advances.sciencemag.org/content/suppl/2019/12/20/6.1.eaax6250.DC1>

REFERENCES This article cites 44 articles, 3 of which you can access for free
<http://advances.sciencemag.org/content/6/1/eaax6250#BIBL>

PERMISSIONS <http://www.sciencemag.org/help/reprints-and-permissions>

Use of this article is subject to the [Terms of Service](#)

Science Advances (ISSN 2375-2548) is published by the American Association for the Advancement of Science, 1200 New York Avenue NW, Washington, DC 20005. The title *Science Advances* is a registered trademark of AAAS.

Copyright © 2020 The Authors, some rights reserved; exclusive licensee American Association for the Advancement of Science. No claim to original U.S. Government Works. Distributed under a Creative Commons Attribution NonCommercial License 4.0 (CC BY-NC).